IOP Conf. Series: Materials Science and Engineering **310** (2018) 012100 doi:10.1088/1757-899X/310/1/012100

Performance analysis of smart laminated composite plate integrated with distributed AFC material undergoing geometrically nonlinear transient vibrations

Shivakumar J[1], Ashok M H[2], Vishwanath Khadakbhavi[2], Sanjay Pujari[3], Santosh Nandurkar[4]

[1]Principal, Chhattisgarh Engineering College, Durg, Chhattisgarh, India
[2]Faculty,Mechanical Engineering department, Angadi Institute of Technology & Management, Belagavi, Karnataka, India
[3]Principal, Angadi Institute of Technology & Management, Belagavi, Karnataka, India
[4]Faculty, Mechanical Engineering department, KLECET, Belagavi, Karnataka, India

E-mail: vishi_mk@yahoo.co.in

Abstract. The present work focuses on geometrically nonlinear transient analysis of laminated smart composite plates integrated with the patches of Active fiber composites (AFC) using Active constrained layer damping (ACLD) as the distributed actuators. The analysis has been carried out using generalised energy based finite element model. The coupled electromechanical finite element model is derived using Von Karman type nonlinear strain displacement relations and a first-order shear deformation theory (FSDT). Eight-node iso-parametric serendipity elements are used for discretization of the overall plate integrated with AFC patch material. The viscoelastic constrained layer is modelled using GHM method. The numerical results shows the improvement in the active damping characteristics of the laminated composite plates over the passive damping for suppressing the geometrically nonlinear transient vibrations of laminated composite plates with AFC as patch material.

1 Introduction

Few decades back there has been improvement in the design of lightweight and flexible structures, laminated composite structures in the form of beams, plates and shells are being widely used in a large variety of engineering applications in aeronautical, mechanical, civil, chemical and other industries over the past few decades. These laminated composite materials are susceptible to large vibrations with long decay time because of their flexibility and low internal damping. Often structural fatigue and instability are the results of vibrations which lead to a serious deterioration of the structural performance induced by mechanical, thermal, hygrothermal or combined hygro-thermo-mechanical loading. There are many types of useful active materials, such as shape memory alloys, electrostrictives, magnetostrictives, electro rheological fluids etc. Piezoelectric are the most popular smart material for adding smartness to the structures [1]. Piezoceramics have a high structural stiffness, which affords them a strong, voltage dependent actuation authority [2].

The research on smart structures is concerned with the analytical solutions of piezoelectric laminated plate is carried out [3-6]. Exact analysis for static response of cross ply laminated smart shells with nonlinear deformations of piezoelectric composite beams with electromechanical

coupling [7-10]. Finite element analysis of laminate with piezoelectric sensors and actuators is performed [11]. Nonlinear vibration Analysis for transient vibrations of piezoelectric fiber-reinforced laminated composite beams is carried out [12-15].

2 Finite Element Model

A smart rectangular laminated composite plate composed of **N** layer of orthotropic layers is described in **figure 1**. Four rectangular patches of ACLD treatment are placed on top surface and are placed centrally on the substrate plate. The constraining layer of ACLD treatment is made of the AFC material. The thickness of AFC layer is considered as $\mathbf{h_p}$ and that of viscoelastic constrained layer of the ACLD is denoted by $\mathbf{h_v}$. The length and width of the plate are denoted by $\mathbf{a/2, b/2}$ respectively.

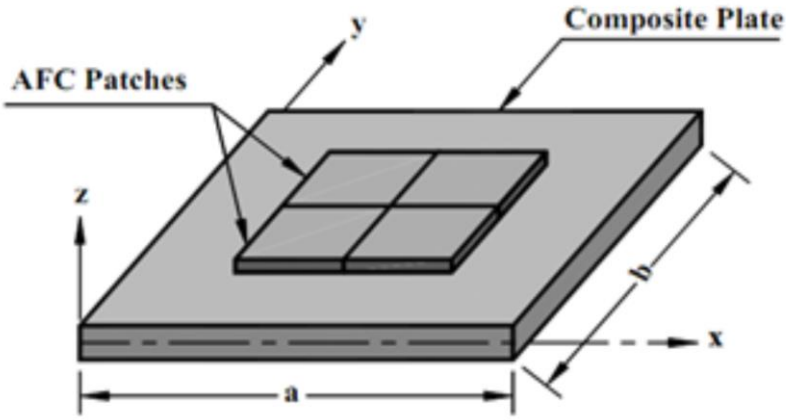

Figure 1. Schematic diagram of smart laminated composite plates Integrated with the patches of AFC material in different configurations

The mid-plane of the substrate plate is considered as the reference plane. The origin of the laminate co-ordinate system $\mathbf{(x, y, z)}$ is chosen on the reference plane in such a way that the boundaries of the overall plate coincide with the line $\mathbf{x = 0, a}$ and $\mathbf{y = 0, b}$. Also, $\mathbf{h_{k+1}}$ and $\mathbf{h_k}$ are the thickness co-ordinate $\mathbf{z}$ of the top and bottom surfaces of any layer respective where $\mathbf{k}$ is the layer number. In any layer of the substrate plate the fiber orientation angle with respect to the laminate coordinate system is denoted by $\boldsymbol{\theta}$. In case of constraining AFC layer of the patches the orientation of fibers with respect to laminate coordinate system is denoted by $\boldsymbol{\psi}$. The fibers are longitudinally aligned in the plane of the AFC layer parallel to $\mathbf{xy}$ plane.

The axial displacements for modelling the kinematics of deformations of the plate coupled with the ACLD treatment are considered based on the FSDT. The schematic representations of the kinematics based on FSDT are illustrated in **figure 2** and **3**. Where, $\mathbf{u_0}$ and $\mathbf{v_0}$ are the generalized translational displacements of reference point $\mathbf{(x, y)}$ on the mid-plane $\mathbf{(z = 0)}$ of the substrate composite plate along **x** and **y** axes respectively θ_x, ϕ_x and γ_x are generalized rotations of the normal to the middle plane of the substrate, the viscoelastic layer and the AFC layer, respectively about **y**-axis. Similarly θ_y, ϕ_y and γ_y are generalized rotations of the about $\mathbf{x}$ - axis. As per **figure 2 and 3** the displacements $\mathbf{u}$ and $\mathbf{v}$ at a point in any layer of the overall plate along $\mathbf{x}$ and $\mathbf{y}$ directions, respectively can be given by,

$$\mathbf{u(x,y,z,t)=u_0(x,y,t)+\left(z-\left\langle z-\frac{h}{2}\right\rangle\right)\theta_x(x,y,t)+\left(\left\langle z-\frac{h}{2}\right\rangle-\langle z-h_{N+2}\rangle\right)\phi_x(x,y,t)+\langle z-h_{N+2}\rangle\gamma_x(x,y,t)} \tag{2.1}$$

$$\mathbf{v(x,y,z,t)=v_0(x,y,t)+\left(z-\left\langle z-\frac{h}{2}\right\rangle\right)\theta_y(x,y,t)+\left(\left\langle z-\frac{h}{2}\right\rangle-\langle z-h_{N+2}\rangle\right)\phi_y(x,y,t)+\langle z-h_{N+2}\rangle\gamma_y(x,y,t)} \tag{2.2}$$

$$\mathbf{w(x,y,z,t)=w_0(x,y,t)+\left(z-\left\langle z-\frac{h}{2}\right\rangle\right)\theta_z(x,y,t)+\left(\left\langle z-\frac{h}{2}\right\rangle-\langle z-h_{N+2}\rangle\right)\phi_z(x,y,t)+\langle z-h_{N+2}\rangle\gamma_z(x,y,t)} \tag{2.3}$$

In which, a function within the bracket $\langle\ \rangle$ represents the appropriate singularity functions for satisfying the continuity conditions between any two continua.

For the simplification of the analysis, the generalized displacement variables are separated into translational $\{\mathbf{d_t}\}$ and rotational $\{\mathbf{d_r}\}$ variables as follows:

$$\{\mathbf{d}\}=\{\mathbf{d_t}\}+[\mathbf{z}]\{\mathbf{d_r}\} \tag{2.4}$$

Where, $\{\mathbf{d}\}=[\mathbf{u\ v\ w}]^{\mathbf{T}}$, $\{\mathbf{d_t}\}=[\mathbf{u_0\ v_0\ w_0}]^{\mathbf{T}}$ and $\{\mathbf{d_r}\}=[\boldsymbol{\theta}_x\ \boldsymbol{\theta}_y\ \boldsymbol{\theta}_y\ \boldsymbol{\phi}_x\ \boldsymbol{\phi}_y\ \boldsymbol{\phi}_z\ \boldsymbol{\gamma}_x\ \boldsymbol{\gamma}_y\ \boldsymbol{\gamma}_z]^{\mathbf{T}}$

In order to implement the selective integration rule for avoiding the shear locking in thin plates and for computing the element stiffness matrices corresponding to the transverse shear deformations, the state of strain at any point in the overall plate is divided into the following two strain vectors i.e. in-plane strains $\{\boldsymbol{\varepsilon}_b\}$ and transverse shear strains $\{\boldsymbol{\varepsilon}_{sh}\}$ and

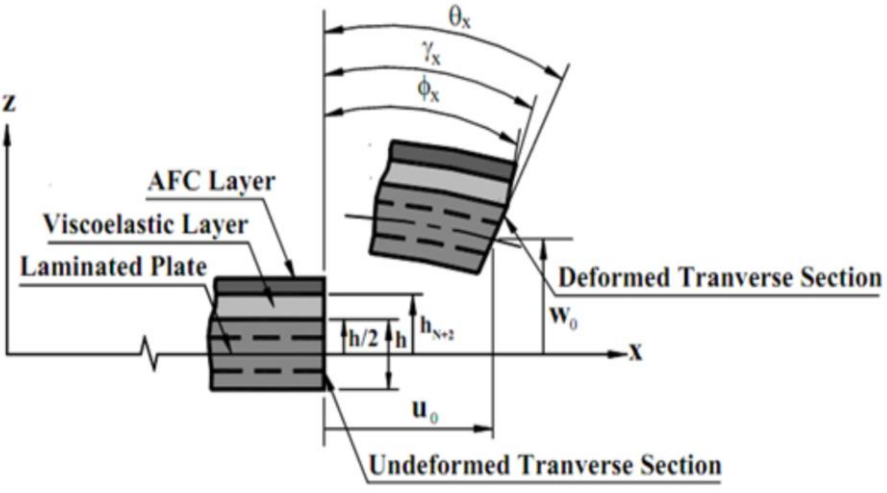

Figure 2. Deformation of any transverse cross-section of the laminated plate Integrated with the ACLD treatment which is parallel to yz plane.

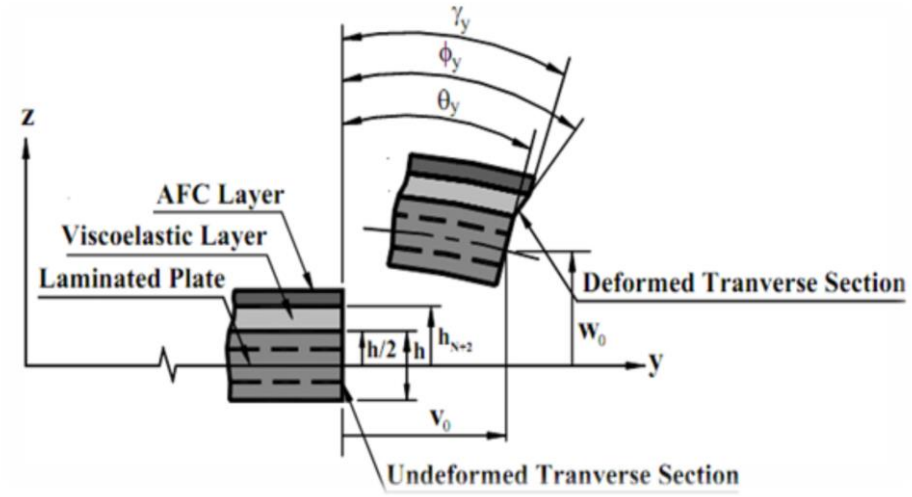

Figure 3. Deformation of any transverse cross-section of the laminated plate Integrated with the ACLD treatment which is parallel to xz plane

are given by Eq. 2.5, similarly, state of stress is plate is given by following two stress vectors i.e. in-plane stress $\{\sigma_b\}$ and transverse shear stress $\{\sigma_{sh}\}$ and are expressed by Eq. 2.6.

$$\{\varepsilon_b\}=[\varepsilon_x\ \varepsilon_y\ \varepsilon_{xy}\ \varepsilon_z]^T \text{ and } \{\varepsilon_{sh}\}=[\varepsilon_{xz}\ \varepsilon_{yz}]^T \tag{2.5}$$

$$\{\sigma_b\}=[\sigma_x\ \sigma_y\ \sigma_{xy}\ \sigma_z]^T \text{ and } \{\sigma_{sh}\}=[\sigma_{xz}\ \sigma_{yz}]^T \tag{2.6}$$

The electric field in the AFC patches is considered to act only in the z and x directions respectively. Hence for the laminated composite plate coupled with the patches of the ACLD treatment the total potential energy T_P and the kinetic energy T_K can be expressed as,

$$T_P = \frac{1}{2}\left[\sum_{k=1}^{N+2}\int_{\Omega_k}(\{\varepsilon_b{}^k\}^T\{\sigma_b{}^k\}+\{\varepsilon_{sh}^k\}^T\{\sigma_{sh}^k\})d\Omega - \int_{\Omega_{N+2}} E_i D_i dv\right] - \int_A pwdA \tag{2.7}$$

$$T_k = \frac{1}{2}\left[\sum_{k=1}^{N+2}\int_{\Omega_k}\rho^k\left(\dot{u}^2+\dot{v}^2+\dot{w}^2\right)d\Omega\right] \tag{2.8}$$

Where, p is externally applied transversely distributed load acting over a surface area A, Ω_k and ρ^k represent the volume and mass density of the k^{th} layer. The subscript $i = x$ for AFC and z for PFRC material. The value of the k is 1 to N for substrate, $N+1$ for viscoelastic layer, $N+2$ for the AFC layer and the dot (˙) over the variables denoted the derivative of respective variable with respect to time.

The constitutive relations for the orthotropic layers of the substrate plate are given by,

$$\{\sigma_b^k\}=[C_b^k]\{\varepsilon_b^k\} \text{ and } \{\sigma_{sh}^k\}=[C_{sh}^k]\{\varepsilon_{sh}^k\}\ \text{k=1,2,3,……N} \tag{2.9}$$

$$\text{Where } \left[\mathbf{C_b^k}\right] = \begin{bmatrix} \mathbf{C_{11}^k} & \mathbf{C_{12}^k} & \mathbf{C_{16}^k} & \mathbf{C_{13}^k} \\ \mathbf{C_{12}^k} & \mathbf{C_{22}^k} & \mathbf{C_{26}^k} & \mathbf{C_{23}^k} \\ \mathbf{C_{16}^k} & \mathbf{C_{26}^k} & \mathbf{C_{66}^k} & \mathbf{C_{36}^k} \\ \mathbf{C_{13}^k} & \mathbf{C_{23}^k} & \mathbf{C_{36}^k} & \mathbf{C_{33}^k} \end{bmatrix}, \left[\mathbf{C_s^k}\right] = \begin{bmatrix} \mathbf{C_{55}^k} & \mathbf{C_{45}^k} \\ \mathbf{C_{45}^k} & \mathbf{C_{44}^k} \end{bmatrix}$$

The material used for viscoelastic layer is assumed to be isotropic and behaves linearly. The constitutive relation for the time domain analysis of the overall plate undergoing ACLD treatment can be given by the Stieltjes integral [1].

$$\left\{\boldsymbol{\sigma}_{\mathbf{sh}}\right\}^{\mathbf{N+1}} = \int_0^{\mathbf{t}} \mathbf{G(t-\tau)} \frac{\partial \left\{\boldsymbol{\varepsilon}_{\mathbf{sh}}\right\}_{\mathbf{v}}}{\partial \boldsymbol{\tau}} \partial \boldsymbol{\tau} \tag{2.10}$$

where, $\mathbf{G(t)}$ is relaxation function of viscoelastic material. Eight noded iso-parametric elements are used to discretize the overall plate. Now utilizing the constitutive relations given by Eq. 2.9, the total potential energy $\mathbf{T_P^e}$ of a typical element integrated with the patch of AFC material using ACLD treatment is given by

$$\begin{aligned} \mathbf{T_P^e} = \frac{1}{2}[&\{\mathbf{d_t^e}\}^{\mathbf{T}}[\mathbf{K_{tt}^e}]\{\mathbf{d_t^e}\} + \{\mathbf{d_t^e}\}^{\mathbf{T}}[\mathbf{K_{tr}^e}]\{\mathbf{d_t^e}\} + \{\mathbf{d_r^e}\}^{\mathbf{T}}[\mathbf{K_{tr}^e}]\{\mathbf{d_t^e}\} + \{\mathbf{d_t^e}\}^{\mathbf{T}}[\mathbf{K_{rr}^e}]\{\mathbf{d_t^e}\} \\ &+ \{\mathbf{d_t^e}\}^{\mathbf{T}}[\mathbf{K_{tsv}^e}]\int_0^{\mathbf{t}} \mathbf{G(t-\tau)} \frac{\partial}{\partial \boldsymbol{\tau}}\{\mathbf{d_t^e}\}\partial\boldsymbol{\tau} + \{\mathbf{d_t^e}\}^{\mathbf{T}}[\mathbf{K_{trsv}^e}]\int_0^{\mathbf{t}} \mathbf{G(t-\tau)} \frac{\partial}{\partial \boldsymbol{\tau}}\{\mathbf{d_r^e}\}\partial\boldsymbol{\tau} \\ &+ \{\mathbf{d_r^e}\}^{\mathbf{T}}[\mathbf{K_{trsv}^e}]\int_0^{\mathbf{t}} \mathbf{G(t-\tau)} \frac{\partial}{\partial \boldsymbol{\tau}}\{\mathbf{d_t^e}\}\partial\boldsymbol{\tau} + \{\mathbf{d_r^e}\}^{\mathbf{T}}[\mathbf{K_{rrsv}^e}]\int_0^{\mathbf{t}} \mathbf{G(t-\tau)} \frac{\partial}{\partial \boldsymbol{\tau}}\{\mathbf{d_r^e}\}\partial\boldsymbol{\tau} \\ &- \{\mathbf{d_t^e}\}\{\mathbf{F_{tpn}^e}\}\mathbf{V} - 2\{\mathbf{d_t^e}\}\{\mathbf{F_{tbp/a}^e}\} - 2\{\mathbf{d_r^e}\}\{\mathbf{F_{rbp/a}^e}\} - \left\{\mathbf{d_t^e}\right\}^{\mathbf{T}}\left[\mathbf{F_{tt}^e}\right] - \left\{\mathbf{d_r^e}\right\}^{\mathbf{T}}\left[\mathbf{F_{rt}^e}\right] \\ &- \frac{\boldsymbol{\varepsilon}_{33}\mathbf{V}^2}{\mathbf{d_p^2}} - 2\{\mathbf{d_t^e}\}\{\mathbf{F^e}\}] \end{aligned} \tag{2.11}$$

In the expression for $\mathbf{T_P^e}$ given in Eq.2.11, $\mathbf{V}$ is voltage difference applied between the electrodes for AFC of the patch of ACLD treatment such that $\mathbf{E_i} = -\frac{\mathbf{V}}{\mathbf{h_p}}$ (where $\mathbf{i} = \mathbf{x}$ for AFC). The element stiffness matrices $\left[\mathbf{K_{tt}^e}\right]$, $\left[\mathbf{K_{tr}^e}\right]$, $\left[\mathbf{K_{rt}^e}\right]$, $\left[\mathbf{K_{rr}^e}\right]$, $\left[\mathbf{K_{tsv}^e}\right]$, $\left[\mathbf{K_{trsv}^e}\right]$, $\left[\mathbf{K_{rrsv}^e}\right]$, element electro-elastic coupling vectors $\left\{\mathbf{F_{tpn}^e}\right\}$, $\left\{\mathbf{F_{tbp/a}^e}\right\}$, $\left\{\mathbf{F_{rbp/a}^e}\right\}$ and element load vector $\left\{\mathbf{F^e}\right\}$ are given by

$$[\mathbf{K_{tb}^e}] = \int_{0.}^{\mathbf{a_e}}\int_{0}^{\mathbf{b_e}} [\mathbf{B_{tb}}]^{\mathbf{T}}[\mathbf{D_{tb}}][\mathbf{B_{tb}}]\mathbf{dxdy}\,, [\mathbf{K_{tbp}^e}] = \int_{0.}^{\mathbf{a_e}}\int_{0}^{\mathbf{b_e}} [\mathbf{B_{tb}}]^{\mathbf{T}}[\mathbf{D_{tbp}}][\mathbf{B_{tb}}]\mathbf{dxdy}\,,$$

$$[\mathbf{K_{trb}^e}] = \int_{0.}^{\mathbf{a_e}}\int_{0}^{\mathbf{b_e}} [\mathbf{B_{tb}}]^{\mathbf{T}}\left[[\mathbf{D_{trb}}]\right][\mathbf{B_{rb}}]\mathbf{dxdy}\,, [\mathbf{K_{rrb}}] = \int_{0.}^{\mathbf{a_e}}\int_{0}^{\mathbf{b_e}} [\mathbf{B_{rb}}]^{\mathbf{T}}\left[[\mathbf{D_{rrb}}]\right][\mathbf{B_{rb}}]\mathbf{dxdy}$$

$$[\mathbf{K_{trbp}^e}] = \int_{0.}^{\mathbf{a_e}}\int_{0}^{\mathbf{b_e}} [\mathbf{B_{tb}}]^{\mathbf{T}}\left[[\mathbf{D_{trb}}]_{\mathbf{p/a}}\right][\mathbf{B_{rb}}]\mathbf{dxdy}\,, [\mathbf{K_{rrb}}]_{\mathbf{p}} = \int_{0.}^{\mathbf{a_e}}\int_{0}^{\mathbf{b_e}} [\mathbf{B_{rb}}]^{\mathbf{T}}\left[[\mathbf{D_{rrb}}]_{\mathbf{p/a}}\right][\mathbf{B_{rb}}]\mathbf{dxdy}$$

$$\{\mathbf{F^e}\}=\int_0^{a_e}\int_0^{b_e}[\mathbf{N_t}]^T\{\mathbf{f}\}\mathbf{dxdy}\ ,\ \{\mathbf{F^e_{tp}}\}=\int_0^{a_e}\int_0^{b_e}[\mathbf{B_{tb}}]^T(-\int_{h_{N+2}}^{h_{N+3}}\frac{\{\bar{\mathbf{e}}\}}{\mathbf{h_p}}\mathbf{dz})\mathbf{dxdy}$$

$$\{\mathbf{F^e_{rp}}\}=\int_0^{a_e}\int_0^{b_e}[\mathbf{B_{rb}}]^T(-\int_{h_{N+2}}^{h_{N+3}}\frac{[\mathbf{z}_3]}{\mathbf{h_p}}\{\bar{\mathbf{e}}\}\mathbf{dz})\mathbf{dxdy}\ ,$$

$$\left\{\mathbf{F^e_{tt}}\right\}=\int_0^{b_e}\int_0^{a_e}\left(\left[\mathbf{B_{tb}}\right]^T\left\{\mathbf{P_{tb}}\right\}\right)\mathbf{dxdy}\ \left\{\mathbf{F^e_{rt}}\right\}=\int_0^{b_e}\int_0^{a_e}\left(\left[\mathbf{B_{rb}}\right]^T\left\{\mathbf{P_{rb}}\right\}\right)\mathbf{dxdy}\ ,\ [\mathbf{K^e_{ts}}]=\int_0^{a_e}\int_0^{b_e}[\mathbf{B_{ts}}]^T[\mathbf{D_{ts}}][\mathbf{B_{ts}}]\mathbf{dxdy}$$

$$[\mathbf{K^e_{trs}}]=\int_0^{a_e}\int_0^{b_e}[\mathbf{B_{ts}}]^T\left[[\mathbf{D_{trs}}]\right][\mathbf{B_{rs}}]\mathbf{dxdy}\ ,\ [\mathbf{K_{rrs}}]=\int_0^{a_e}\int_0^{b_e}[\mathbf{B_{rs}}]^T\left[[\mathbf{D_{rrs}}]\right][\mathbf{B_{rs}}]\mathbf{dxdy}$$

$$[\mathbf{K^e_{tsp}}]=\int_0^{a_e}\int_0^{b_e}[\mathbf{B_{ts}}]^T[\mathbf{D_{tsp}}][\mathbf{B_{ts}}]\mathbf{dxdy}\ ,\ [\mathbf{K^e_{trsp}}]=\int_0^{a_e}\int_0^{b_e}[\mathbf{B_{ts}}]^T\left[[\mathbf{D_{trs}}]_{\mathbf{p/a}}\right][\mathbf{B_{rs}}]\mathbf{dxdy}$$

$$[\mathbf{K_{rrs}}]_{\mathbf{p}}=\int_0^{a_e}\int_0^{b_e}[\mathbf{B_{rs}}]^T\left[[\mathbf{D_{rrs}}]_{\mathbf{p/a}}\right][\mathbf{B_{rs}}]\mathbf{dxdy}\ ,\ [\mathbf{K^e_{tsv}}]=\mathbf{h_v}\int_0^{a_e}\int_0^{b_e}[\mathbf{B_{ts}}]^T[\mathbf{B_{ts}}]\mathbf{dxdy}$$

$$[\mathbf{K^e_{trsv}}]=\mathbf{h_v}\int_0^{a_e}\int_0^{b_e}[\mathbf{B_{ts}}]^T[\mathbf{Z}_5][\mathbf{B_{rs}}]\mathbf{dxdy}\ ,\ [\mathbf{K^e_{rrsv}}]=\mathbf{h_v}\int_0^{a_e}\int_0^{b_e}[\mathbf{B_{rs}}]^T[\mathbf{Z}_5]^T[\mathbf{Z}_5][\mathbf{B_{rs}}]\mathbf{dxdy}\quad(2.12)$$

where, $\mathbf{a_e}$ and $\mathbf{b_e}$ are the length and width of the element under consideration and the various rigidity matrices originated in the above elemental matrices.

The expression for kinetic energy $\mathbf{T^e_k}$ of the element is given by,

$$\mathbf{T^e_k}=\frac{1}{2}\{\dot{\mathbf{d}}^{\mathbf{e}}_{\mathbf{t}}\}[\mathbf{M^e}]\{\dot{\mathbf{d}}^{\mathbf{e}}_{\mathbf{t}}\}\quad(2.13)$$

in which

$$[\mathbf{M^e}]=\int_0^{a_e}\int_0^{b_e}\bar{\mathbf{m}}\{\mathbf{N_t}\}^T\left[\mathbf{N_t}\right]\mathbf{dxdy}\ \text{and}\ \bar{\mathbf{m}}=\sum_{\mathbf{k}=1}^{\mathbf{N}}\boldsymbol{\rho}^{\mathbf{k}}(\mathbf{h_{k+1}}-\mathbf{h_k})+\boldsymbol{\rho}^{\mathbf{N+1}}(\mathbf{h_v})+\boldsymbol{\rho}^{\mathbf{N+2}}(\mathbf{h_p})$$

As the thickness of the substrate plate is less, the rotary inertia of the overall plate has been neglected while calculating the kinetic energy of the plate. Using principle of virtual work, the following governing equations of motion of an element are obtained:

$$\begin{aligned}&[\mathbf{M^e}]\{\ddot{\mathbf{d}}^{\mathbf{e}}_{\mathbf{t}}\}+[\mathbf{k^e_{tt}}]\{\mathbf{d^e_t}\}+[\mathbf{k^e_{tr}}]\{\mathbf{d^e_r}\}+[\mathbf{k^e_{tsv}}]\int_0^{\mathbf{t}}\mathbf{G(t-\tau)}\frac{\partial}{\partial\boldsymbol{\tau}}\{\mathbf{d^e_t}\}\partial\boldsymbol{\tau}\\&+[\mathbf{k^e_{trsv}}]\int_0^{\mathbf{t}}\mathbf{G(t-\tau)}\frac{\partial}{\partial\boldsymbol{\tau}}\{\mathbf{d^e_r}\}\partial\boldsymbol{\tau}=\{\mathbf{F^e}\}+\left[\{\mathbf{F^e_{tbp/a}}\}+\{\mathbf{F^e_{rbp/a}}\}\right]\mathbf{V}+\left\{\mathbf{F_{tt}}\right\}\end{aligned}\quad(2.14)$$

and

$$[\mathbf{k}^{e}_{rt}]\{\ddot{\mathbf{d}}^{e}_{t}\}+[\mathbf{k}^{e}_{rr}]\{\mathbf{d}^{e}_{r}\}+[\mathbf{k}^{e}_{trsv}]^{T}\int_{0}^{t}\mathbf{G}(t-\tau)\frac{\partial}{\partial\tau}\{\mathbf{d}^{e}_{t}\}\partial\tau$$
$$+[\mathbf{k}_{rrsv}]\int_{0}^{t}\mathbf{G}(t-\tau)\frac{\partial}{\partial\tau}\{\mathbf{d}^{e}_{r}\}\partial\tau=\{\mathbf{F}_{rbp/a}\}\mathbf{V}+\{\mathbf{F}_{tr}\} \quad (2.15)$$

The values of $\{\mathbf{F}^{e}_{tpn}\}$, $\{\mathbf{F}^{e}_{tbp/a}\}$, and $\{\mathbf{F}^{e}_{rbp/a}\}$ will be zero for an element without integrated ACLD patch. On assembly the elemental equations turn out to be Global equations of motion which are given by

$$[\mathbf{M}]\{\ddot{\mathbf{X}}_{t}\}+[\mathbf{K}_{tt}]\{\mathbf{X}_{t}\}+[\mathbf{K}_{tr}]\{\mathbf{X}_{r}\}+[\mathbf{K}_{tsv}]\int_{0}^{t}\mathbf{G}(t-\tau)\frac{\partial}{\partial\tau}\{\mathbf{X}_{t}\}\partial\tau$$
$$+[\mathbf{K}_{trsv}]\int_{0}^{t}\mathbf{G}(t-\tau)\frac{\partial}{\partial\tau}\{\mathbf{X}_{r}\}\partial\tau=\{\mathbf{F}\}+\left[\{\mathbf{F}_{tpn}\}+\{\mathbf{F}_{tp}\}\right]\mathbf{V}+\{\mathbf{F}_{tt}\} \quad (2.16)$$

$$[\mathbf{K}_{rt}]\{\mathbf{X}_{t}\}+[\mathbf{K}_{rr}]\{\mathbf{X}_{r}\}+[\mathbf{K}_{trsv}]\int_{0}^{t}\mathbf{G}(t-\tau)\frac{\partial}{\partial\tau}\{\mathbf{X}_{t}\}\mathbf{d}\tau$$
$$+[\mathbf{K}_{rrsv}]\int_{0}^{t}\mathbf{G}(t-\tau)\frac{\partial}{\partial\tau}\{\mathbf{X}_{r}\}\mathbf{d}\tau=\{\mathbf{F}_{rp}\}\mathbf{V}+\{\mathbf{F}_{tr}\} \quad (2.17)$$

in which $[\mathbf{M}]$ is the global mass matrix, $[\mathbf{K}_{tt}]$, $[\mathbf{K}_{tr}]$, $[\mathbf{K}_{rt}]$, $[\mathbf{K}_{rr}]$, $[\mathbf{K}_{tsv}]$, $[\mathbf{K}_{trsv}]$, $[\mathbf{K}_{rrsv}]$ are global stiffness matrices, $\{\mathbf{F}_{tpn}\},\{\mathbf{F}_{tp}\},\{\mathbf{F}_{rp}\}$ are global electroelastic coupling vectors, $\{\mathbf{F}_{tt}\}$, $\{\mathbf{F}_{tr}\}$ are thermal related force vectors, $\{\mathbf{X}_{t}\}$, $\{\mathbf{X}_{r}\}$ are global nodal generalized displacement vectors, $\{\mathbf{F}\}$ is the global nodal mechanical force vector. The element stiffness matrices $[\mathbf{K}_{tt}]$, $[\mathbf{K}_{tr}]$ are quadratic in displacement variables. Thus the global equations of motion given by Eqs. 2.16 and 2.17 turn out to be nonlinear, where $\{\tilde{\mathbf{Z}}_{t}(\mathbf{s})\}$ and $\{\tilde{\mathbf{Z}}_{r}(\mathbf{s})\}$ are the Laplace transforms of $\{\mathbf{Z}_{t}\}$ and $\{\mathbf{Z}_{r}\}$ respectively. Using time domain representation of the auxiliary dissipation coordinates equation of governing coupled electro-elastic open loop behaviour of laminated composite plate integrated with the patches of ACLD treatment can be represented by

$$[\mathbf{M}^{*}]\{\ddot{\mathbf{X}}\}+[\mathbf{C}^{*}]\{\dot{\mathbf{X}}\}+[\mathbf{K}^{*}]\{\mathbf{X}\}=\{\mathbf{F}^{*}\}+\{\mathbf{F}^{*}_{p}\}\mathbf{V}+\{\mathbf{F}_{t}\} \quad (2.18)$$

in which

$$[\mathbf{M}^{*}]=\begin{bmatrix}[\mathbf{M}] & 0 & 0\\ 0 & \mathbf{I}_{z} & 0\\ 0 & 0 & \mathbf{I}_{zr}\end{bmatrix},[\mathbf{K}^{*}]=\begin{bmatrix}[\mathbf{K}_{x}] & [\mathbf{K}_{z}] & [\mathbf{K}_{zr}]\\ -\hat{\omega}^{2}\mathbf{I}_{z} & \hat{\omega}^{2}\mathbf{I}_{z} & 0\\ \hat{\omega}^{2}[\mathbf{K}_{1}] & -\hat{\omega}^{2}[\mathbf{K}_{2}] & \hat{\omega}^{2}[\mathbf{K}_{3}]\end{bmatrix},\ [\mathbf{C}^{*}]=\begin{bmatrix}0 & 0 & 0\\ 0 & 2\xi\hat{\omega} & 0\\ 0 & 0 & 2\xi\hat{\omega}\end{bmatrix}$$
$$[\mathbf{X}]=\begin{bmatrix}\{\mathbf{X}_{t}\}\\ \{\mathbf{Z}_{t}\}\\ \{\mathbf{Z}_{r}\}\end{bmatrix},\ [\mathbf{F}^{*}]=\begin{Bmatrix}\{\tilde{\mathbf{F}}\}\\ 0\\ 0\end{Bmatrix},\ [\mathbf{F}^{*}_{p}]=\begin{Bmatrix}\{\mathbf{F}_{p}\}\\ 0\\ \{\mathbf{F}_{pz}\}\end{Bmatrix},\{\mathbf{F}_{t}\}=\{\mathbf{F}_{tt}\}-[\mathbf{K}_{tr}][\mathbf{K}_{rr}]^{-1}\{\mathbf{F}_{tr}\}^{T} \quad (2.19)$$

Where, $\mathbf{I}_{z}$ and $\mathbf{I}_{zr}$ are the identity matrices of appropriate sizes associated with the dissipation coordinates, $\{\mathbf{Z}_{t}\}$ and $\{\mathbf{Z}_{r}\}$ respectively.

3. Numerical results:

In order to assess the performance of the ACLD patches made of AFC material in controlling the nonlinear vibrations of laminated composite plates, numerical results are computed using the finite element model. Both symmetric cross-ply and antisymmetric cross-ply thin square substrates integrated with four patches of ACLD treatment (**Figure 1**) is considered for evaluating the numerical results. The elastic and piezoelectric properties of the othotropic layers of substrate plates and the AFC patches are considered for evaluating the numerical results. The thicknesses of the AFC patch, the viscoelastic patch and the laminated plates are considered as **250 μm**, **50.8 μm** and **3 mm**, respectively. Also, the orthotropic layers of the substrate plate are of equal thickness. Unless otherwise mentioned, the piezoelectric fiber orientation angle ψ in the AFC patch is considered to be **0°**. Considering a single term GHM expression, the values of α, $\hat{\xi}$ and $\hat{\omega}$ are used as **11.42**, **1.0261e5**, **20** respectively. The shear modulus G^{∞} and the density of the viscoelastic material ρ_v are **1.822e6 Pa** and **1104 kg/m^3** respectively. The mechanical load **p** acting upward is assumed to be uniformly distributed while the aspect ratio $\mathbf{a/h}$ is considered to be **300**. The boundary conditions used for evaluating the numerical results are considered as follows:

$$\text{Simply supported (SS1): } v_0 = w_0 = \theta_y = \phi_y = \gamma_y = 0 \text{ at } x = 0, a$$
$$u_0 = w_0 = \theta_x = \phi_x = \gamma_x = 0 \text{ at } y = 0, b$$
$$\text{Simply supported (SS2): } v_0 = w_0 = \theta_y = \phi_y = \gamma_y = 0 \text{ at } x = 0, a$$
$$v_0 = w_0 = \theta_x = \phi_x = \gamma_x = 0 \text{ at } y = 0, b$$
$$\text{Clamped (CC): } u_0 = w_0 = \theta_y = \phi_y = \gamma_y = 0 \text{ at } x = 0, a$$
$$u_0 = w_0 = \theta_x = \phi_x = \gamma_x = 0 \text{ at } y = 0, b$$

The open loop and closed-loop behaviour of the substrates are studied by the evaluation of transverse deflection at the centre of the plate $(a/2, b/2, h/2)$ on the top of the substrates. A uniformly distributed transverse pulse step load is applied to set the overall plate into motion. It has been found [8, 9] that if the value of the non-dimensional form $Q = pa^4/(E_T h^4)$ of the applied mechanical load exceeds the value **40**, the overall plate undergoes nonlinear deformations. Hence, for the purpose of computing the nonlinear transient responses, the non-dimensional values of the applied pulse load are considered more than **50**.

Also to validate the present model for open and closed loop nonlinear transient responses using ACLD treatment made of AFC material for smart patches placed at the center and with identical conditions for a simply-supported symmetric cross-ply $(0^o/90^o/0^o)$ square substrate plate, the results shown in **figures 5** and **6** indicate that the results obtained by the present scheme agree in an excellent manner with the existing one. Thus validating the present finite element model with ACLD treatment made of AFC material.

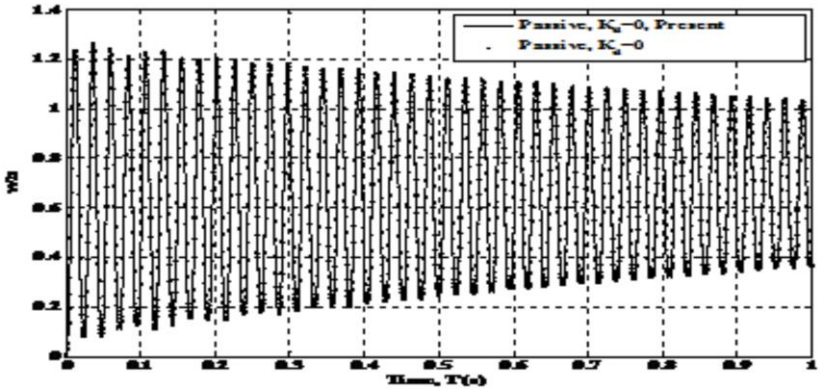

Figure 4. Comparison of present model for Nonlinear dynamic response of a simply- supported (SS1) symmetric cross-ply $(0^o/90^o/0^o)$ square substrate plate undergoing active constrained layer damping (a/h=200 Load=500 N/m^2) using AFC material under passive mode ($K_d=0$)

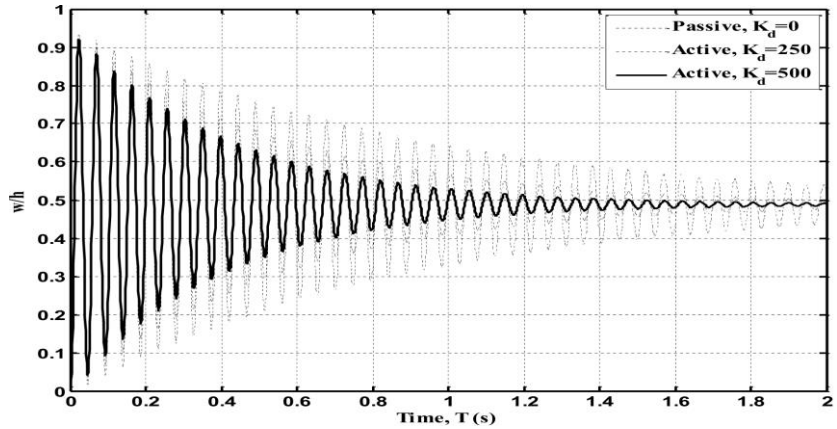

Figure 5. Nonlinear dynamic response of a simply-supported (SS1) symmetric crossply $(0^o/90^o/0^o)$ square substrate plate undergoing active constrained layer damping (for a/h=300 , Q=100) using AFC

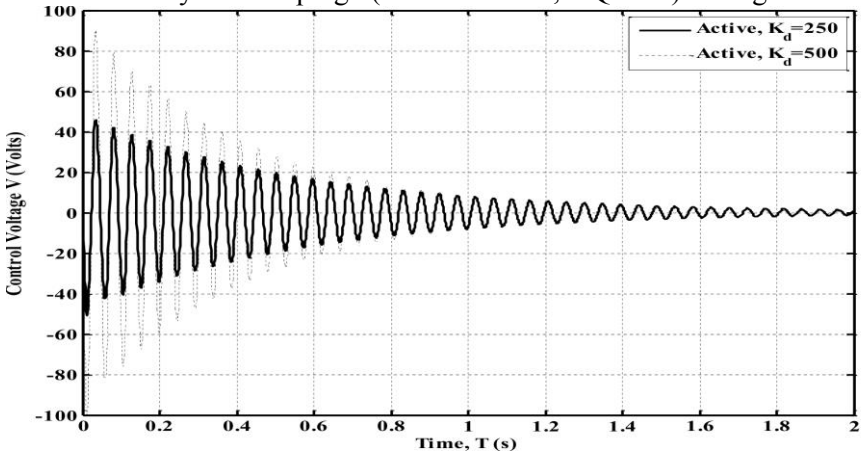

Figure 6. Control voltages required for the active constrained layer damping of nonlinear transient vibrations of the simply supported (SS1) symmetric cross ply $(0^o/90^o/0^o)$ square substrate plate(for a/h=300 ,Q=100) using AFC

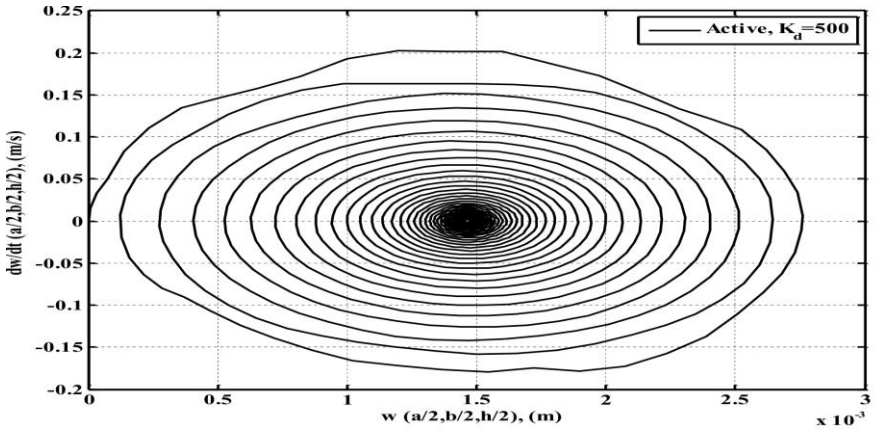

Figure 7. Phase plot of the simply supported (SS1) symmetric cross ply $(0^o/90^o/0^o)$ square substrate plate when the active constrained layer damping patches control the nonlinear vibrations (for a/h=300, Q=100) using AFC

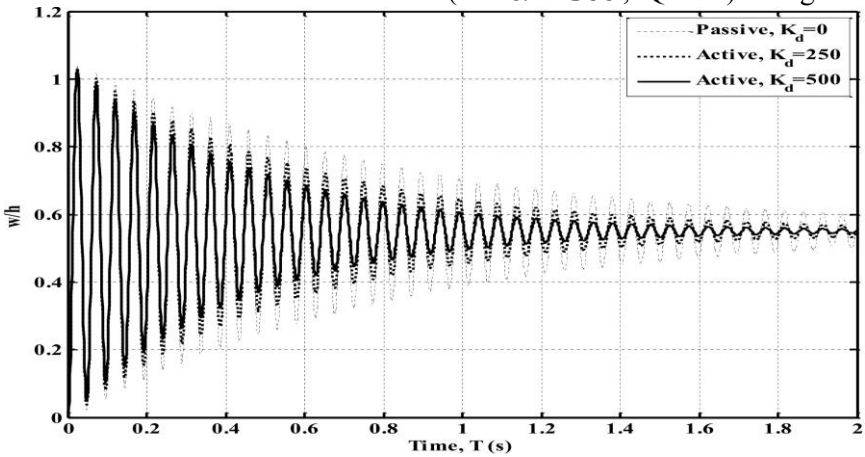

Figure 8. Nonlinear dynamic response of a simply-supported (SS1) symmetric cross-ply $(0^o/90^o/0^o/90^o)$ square substrate plate undergoing active constrained layer damping (for a/h=300, Q = 100) using AFC

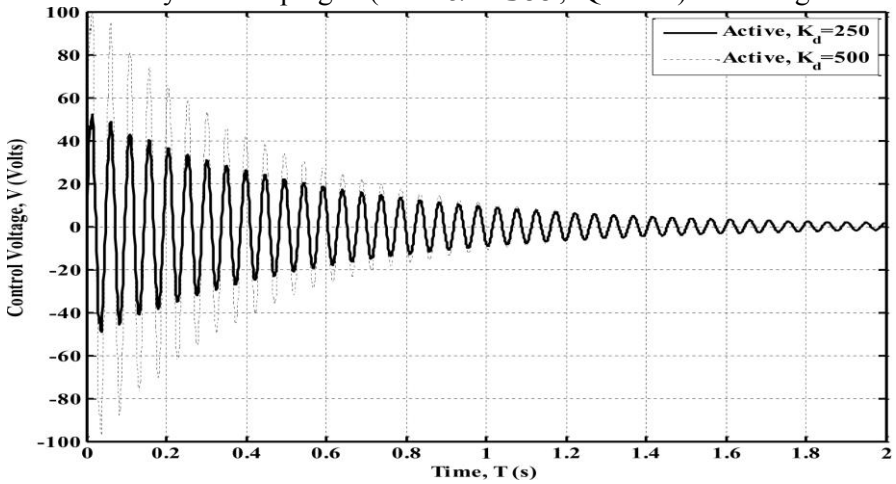

Figure 9. Control voltages required for the active constrained layer damping of nonlinear transient vibrations of the simply supported (SS1) symmetric cross ply $(0^o/90^o/0^o/90^o)$ square substrate plate (for a/h=300, Q=100) using AFC

4. Conclusions:

A three dimensional finite element model has been prepared for identifying the performance of AFC material in controlling geometrically nonlinear static deformations of laminated composite plates. The numerical results highlighted that the AFC material shows the improvement in the active damping characteristics of the laminated composite plates over the passive damping for suppressing the geometrically transient vibrations deformations of laminated composite plates.

References:

1. Shivakumar J. and Ray M. C., Nonlinear Analysis of Smart Cross Composite Plates Integrated with a Distributed Piezoelectric Fiber Reinforced Composite Actuator, *Mechanics of Advanced Materials and Structures*, ISSN 1537-6494, vol. 15, No.1, 2008, pp. 40-52.
2. R Suresh Kumar, M C Ray, Smart damping of geometrically nonlinear vibrations of functionally graded sandwich plates using 1–3 piezoelectric composites, *Journal of Mechanics of Advanced Materials and Structures* Vol. 23, 2016 - Issue 6, Pages 652-669.
3. Saroj Kumar Sarangiand Ray M. C., Smart Control Of Nonlinear Vibrations Of Laminated Plates Using Active Fiber Composites, Vol. 12, No. 6, 2012, DOI:10.1142/S0219455412500502
4. Majed A. Majeed, Ayech Benjeddou, Mohammed A. Al-Ajmi, Free vibration analysis of moderately thick asymmetric piezoelectric adaptive cantilever beams using the distributed transfer function approach, *Journal of Sound and Vibration*, Volume 333, Issue 15, 21 July 2014, pp. 3339-3355
5. Seyedeh Marzieh Hosseini, Hamed Kalhori, Alireza Shooshtari, Nima Mahmoodi S., Analytical solution for nonlinear forced response of a viscoelastic piezoelectric cantilever beam resting on a nonlinear elastic foundation to an external harmonic excitation, *Composites Part B: Engineering*, Volume 67, 2014, pp. 464-471
6. Mehran Shahraeeni, Rezgar Shakeri, Seyyed Mohammad Hasheminejad, An analytical solution for free and forced vibration of a piezoelectric laminated plate coupled with an acoustic enclosure, *Computers & Mathematics with Applications*, Volume 69, Issue 11, 2015, pp. 1329-1341
7. Lin Li, Shunhua Yin, Xue Liu, Jun Li, Enhanced electromechanical coupling of piezoelectric system for multimodal vibration, *Mechatronics*, Volume 31, October 2015, pp. 205-214
8. Khdeir A.A., Aldraihem O.J., Exact analysis for static response of cross ply laminated smart shells, *Composite Structures*, Volume 94, Issue 1, 2011, pp. 92-101
9. VahidTajeddini, Anastasia Muliana, Nonlinear deformations of piezoelectric composite beams, *Composite Structures*, Volume 132, 2015, pp. 1085-1093
10. Zhangjian Wu, Chao Han, ZhongrongNiu, A 3D exact analysis of the boundary layer effect of asymmetric piezoelectric laminates with electromechanical coupling, *International Journal of Solids and Structures*, Volume 72, 2015, pp. 118-129
11. Fallah N., Ebrahimnejad M., Finite volume analysis of adaptive beams with piezoelectric sensors and actuators,*Applied Mathematical Modelling*, Volume 38, Issue 2, 2014, pp. 722-737
12. Mareishi S., Rafiee M., He X.Q., Liew K.M., Nonlinear free vibration, postbuckling and nonlinear static deflection of piezoelectric fiber-reinforced laminated composite beams, *Composites Part B: Engineering*, Volume 59, 2014, pp. 123-132
13. Ahmad Eduardo Guennam, Bibiana M. Luccioni, Model for piezoelectric/ferroelectric composites polarized with interdigitated electrodes, *Composite Structures*, Volume 131, 2015, pp. 312-324
14. Milazzo A., Variable kinematics models and finite elements for nonlinear analysis of multilayered smart plates, *Composite Structures*, Volume 122, 2015, pp. 537-545
15. Zhang, Shun-Qi, Li, Ya-Xi, Schmidt, Rüdiger, Active shape and vibration control for piezoelectric bonded composite structures using various geometric nonlinearities, *Composite Structures*, Volume 122, April 2015, pp. 239-249